J Fluoresc (2007) 17:437–443
DOI 10.1007/s10895-007-0190-4

ORIGINAL PAPER

Is Phosphorescence Lifetime an Indicator of Angiogenesis in Cortical Sarcoma?

Yuezhi Li · Tao Xu · Hui Guo · Huiling Yang

Received: 20 November 2006 / Accepted: 3 April 2007 / Published online: 23 May 2007

Abstract In this paper, the oxygen dependent phosphorescence quenching method is proposed to study the correlation between the phosphorescence lifetime and microvessel density in tumors. In the implementation, the S180 transplanted tumor in the mouse is used for the collection of the time-resolved phosphorescence, the tumor microvessel density is measured by immunohistochemical examination of FVIII, the correlation between microvessel density and phosphorescence lifetime is analyzed by multiple regression method. The results show the phosphorescence decay constant measured in tumors is enlarged in the tumor progression. Furthermore, the relative total microvessel area is positively correlative with the phosphorescence lifetime, which is estimated by a two dimension regression equation. It is concluded phosphorescence lifetime is a valuable indicator of angiogenesis during the tumor development.

Keywords Angiogenesis · Microvessel density · Phosphorescence quenching · Pd-TCPP · Phosphorescence lifetime

Y. Li (✉)
College of Engineering and Technology, Shenzhen University, 518060 Shenzhen, China
e-mail: yuezhili@sina.com

T. Xu
Academy of Metrology and Quality Inspection of Shenzhen, 518055 Shenzhen, China

H. Guo
Shenzhen People's Hospital, 518020 Shenzhen, China

H. Yang
Zhongshan University, 510089 Guangzhou, China

Introduction

Angiogenesis is essential for solid tumor growth [1, 2]. It has been suggested that angiogenesis is an early event in tumorigenesis [2, 3] and may facilitate tumor progression and metastasis [4]. As it has been indicated in many studies the mechanisms for promotion of angiogenesis are activated in the early stages of tumor development, investigating its promotion in tumor tissue provide a possibility to report tumor progression at the early stage.

Research in this field has been very active in recent years, Weidner et al. reported that tumor angiogenesis can be measured by determining the microvessel density by immunohistochemical methods [4, 5]. Furthermore, computerized image analysis was introduced as a tool for a more objective histological assessment of neovasculature [6–8].

Different from histological assessment, optical methods have their advantage of non-invasive and simple to implement, they are also favored because of their precision and reliability. Among the optical methods, the frequency-domain fluorescence spectrum has been studied and applied most intensively, i.e., in the fields of expanded skin [9, 10], lung [11], mamma gland [12], gastrointestinal tract [13], gullet [14], brain [15], etc. Fluorescence spectroscopy (FS) and diffuse reflectance spectroscopy (DRS) are the two main frequency-domain fluorescence spectrum methods. Although the FS and DRS methods are relatively simple to implement clinically and are successful at various levels, they are steady-state spectral measurement methods and thus share the intrinsic limitations of this kind of method-intensity dependent. The intensity of the detected fluorescent light is contaminated by light emitted by nonfluorescent light absorbers and scatterers in unpredictable and unquantifiable

ways. [16, 17] As a result, the difference obtained using steady-state measurement methods is less reliable.

The oxygen dependent quenching of phosphorescence is a direct non-invasive optical method for measuring oxygen pressure in tissues [18, 19]. This technique makes use of the ability of oxygen molecules to return from the excited triplet state to the ground state by absorbing energy which would otherwise present as phosphorescence. This quenching process requires collision between oxygen and the excited state molecule. The oxygen pressure can be determined by measuring phosphorescence intensity or phosphorescence lifetime [20].

In this paper, we preferred the latter method, which detect the phosphorescence lifetime parameter by capturing the transient decay of the phosphorescence intensity over time, phosphorescence lifetime is regarded as a reliable and important parameter due to the fact that it does not change with either variation in excitation intensity or optical losses from hemoglobin absorption. In other words, it is intensity independent.

The phosphorescence lifetime is a very useful and reliable parameter for determining the properties of the biological molecules from which the corresponding phosphorescence is emitted. It is also known to be extremely sensitive to the local biochemical environment [16]. It is indicated in some studies that the phosphorescence lifetime is strongly dependent on the surrounding oxygen environment [21, 22]. The oxygen dependence of the phosphorescence lifetime can be described by the Stern-Volmer relationship:

$$\frac{\tau_0}{\tau} = 1 + k_q \tau_0 [O_2] \quad (1)$$

where τ_0 and τ are phosphorescence lifetimes in the absence and in the presence of oxygen concentration $[O_2]$, respectively; k_q is the phosphorescence quenching constant.

Using oxygen-dependent phosphorescence quenching of Pd-meso-tetra(4-carboxyphenyl) porphyrin (PdTCPP), there are already some studies on measurements of oxygen pressure in tumors [23, 24]. However, no one is concerning the investigation of the correlation between phosphorescence lifetime and tumor angiogenesis, which is explored with an in vivo experimental method in this paper. The following describes the rationale behind this work.

In tumor progression, solid tumors are typically characterized by hypoxia [25–27]. Despite continuous angiogenesis, oxygen pressure decreases with increasing tumor size. The hypoxic tumor microenvironment is a stimulus for angiogenesis, up-regulating expression of angiogenic factors such as vascular endothelial growth factor (VEGF) by tumor [28] and stromal [29] cells. So, the oxygen-dependent quenching of phosphorescence proven as a powerful method for measuring oxygen concentrations might give possibility to estimate tumor angiogenesis pending an accurate relationship between phosphorescence lifetime and tumor angiogenesis is determined.

Goal of this study is to validate the phosphorescence quenching method in reporting the tumor angiogenesis promotion, which will be very essential to the diagnoses and cure of tumors. In the implementation, the S180 transplanted tumor in the mouse was used to detect the tumor angiogenesis by immunohistochemical examination and the phosphorescence quenching method is applied to collect phosphorescence lifetime in vivo.

Materials and methods

Experimental setup

Forty KM mice (weight: 20~30 g) from the Experimental Animal Center of Southern Medical University, Guangzhou, China, were tested in the experiment. Animals were housed in cages with free access to food and water. Sarcoma tumor cell suspension $(1–2)\times10^{10}$ cells/l was transplanted into the subcutaneous space of the dorsoscapular region of each mouse. A preliminary experiment suggested the lifetime of S180 transplanted mouse is from 16 to 19 days, thus bearing tumor for 5, 10, 15 days were respectively defined as the early, intermediate and late stages of sarcoma. Accordingly, the mice were randomly divided into five groups: bearing tumor for 5, 7, 10, 12 and 15 days. Each group was used for the experiment under following procedures on the 5th, 7th, 10th, 12th, 15th day, respectively.

Pd-*meso*-tetra (4-carboxyphenyl) porphyrin (Pd-TCPP), purchased from Porphyrin Products (Logan, UT), was used as a 10 μM solution. The compound is dissolved in 0.5% bovine serum albumin (BSA) as a stock solution. The mice were injected with a 10 mg/ml Pd-TCPP solution directly into the whole tumor area at a dose of 2.5 $mgkg^{-1}$. About 3 h after injection, the mice were anaesthetized with 50 $mgkg^{-1}$ sodium pentobarbital. The time-resolved spectra of the tumor area were collected using a homemade instrument described in the following subsection. After the time-resolved detection, the tumors were excised and weighed, and portions of the tumor were fixed in 10% formaldehyde, followed with immunohistochemical staining.

Phosphorescence in vivo measurement

The homemade instrument is designed to excite and detect time-resolved phosphorescence. A kind of bifurcated optical fiber assemblies is applied in the design that have two fibers of the same diameter side-by-side in the common end and a divergence into two separate legs from the

breakout of the assembly, a schematic of the apparatus is shown in Fig. 1. A frequency doubling semiconductor laser, produced by the Biomedical Engineering Department of Tianjin Medical University, Tianjin, China, is used as a 532 nm excitation source. The exported laser has pulse width of 400 μs and pulse energy of 1 mJ.

The output laser is coupled into one leg of the Y-shaped optical fiber assemblies (ThorLabs, Newton, NJ). The assemblies couple the laser light into a single 200 mm optical fiber probe, which is used to excite and detect the phosphorescence in tumor tissue. The phosphorescence collected by the probe is transmitted along the other leg of the assemblies and coupled to a photomultiplier tube (R2228, Hamamatsu, Japan). The phosphorescence is filtered with 630~650 nm band-pass filters (Oriel, Stratford, CT) to subdue scattered excitation light and to limit the spectral width of the detected phosphorescence. The pulse from the photomultiplier tube is then amplified, time delayed, and used as a "start" input to a time-correlated single photon counting card (SPC-630, Becker&Hickl, Germany) operated in reversed "start-stop" mode. The "stop" input is fed from an electronic synchronization pulse of the laser driver.

Phosphorescence measurements were performed at the tumor areas on the mice during the morning of each day. Phosphorescence decay was measured using the single optical fiber. An 18-gauge needle, which was disinfected, was used to guide the optical fiber into the tumor tissue. The background for the time-resolved system is the average of the signal measured with the fiber tip in water and in air. Time-resolved data is fit to a single exponential equation of the form:

$$I(t) = I(0)\exp^{-t/T} + B \quad (2)$$

where $I(t)$ is the phosphorescence intensity at time t, and T is the decay constant of the time-resolved spectrum.

Immunohistochemical staining

Immunohistochemical staining was performed by the SABC method. The primary antibody was rabbit anti-human and mouse factor VIII at a dilution of 1:150, routine paraffin-embedded sections from each specimen were incubated in this primary antibody solution overnight at 4°C, rinsed three times in 0.1 mol/l PBS, Biotinylated goat anti-rabbit IgG was added and the sections were incubated at 37°C for 20 min, rinsed three times in 0.1 mol/l PBS, then incubated with streptavidin biotin complex-peroxidase (SABC) at 37°C for 20 min and rinsed three times in 0.1 mol/l PBS. This was followed by chromogenic reaction with 0.05% DAB plus 0.03% H_2O_2, and counterstaining with hematoxylin.

Digital image analysis

The vascularity was determined from immunohistochemically stained slides of each biopsy specimen using computer image analysis. Slides were examined first under low power (×40 to ×100) to identify the region of highest vessel density (hot spot), The three most vascular areas within the tumor for each slide were selected for the following computer image analysis, in which quantification consisted of the microvessel (MV) counts per image, the average area of MV per image, the average perimeter of MV per image, and the relative area of all MV per image field (%). [30]

Images were captured digitally at a resolution of 512×768×12 pixels using a VarioCam monochrome charge-coupled device (CCD) cooling video camera (JVC Ky-F 30 B 3-CCD, Japan), which was connected to an automatic image analyzer (Kontron IBAS, Germany), working with IBAS software release 2.5. The CCD camera was attached to a Carl Zeiss Axiotro bright-field, high-resolution microscope (Zeiss Co, Germany), utilizing a 40×0.75 numerical aperture objective. Thus, each image field is 0.027322 mm^2.

Manual outlining of microvessels was performed; these processed images were then developed with mathematical morphometry that reduced the full 256-gray-level images to

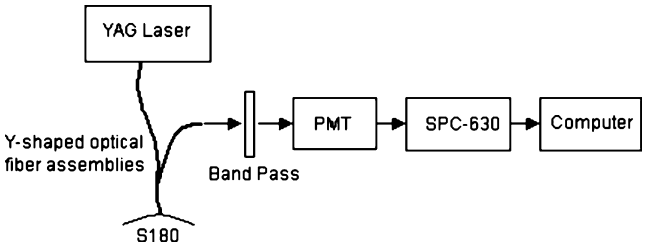

Fig. 1 Experimental apparatus used for phosphorescence lifetime measurements

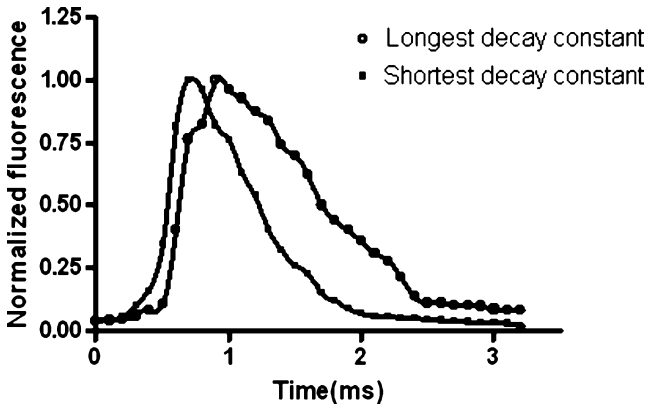

Fig. 2 Representative time-resolved phosphorescence spectra detected in S180 tissue

Table 1 Transplanted S180 tumor weights in different development courses ($x\pm s$)

Course (day)	n		Weight of the mice (g)		Tumor weight (g)
	Beginning	End	Beginning	End	
5	8	8	20.38±1.64	22.52±1.45	0.1301±0.0305
7	8	8	20.23±1.72	23.85±2.65	0.3014±0.0405
10	8	8	20.08±1.51	25.33±3.34	0.5566±0.0885
12	8	8	20.22±1.69	27.74±1.75	1.3033±0.2005
15	8	7	20.01±1.40	30.90±3.08	2.1938±0.3286

Beginning: the day S180 was transplanted; end: the day samples were collected.

binary images, isolated the individual microvessels, and calculated the parameters.

Statistical analysis

Data are reported as mean±SD. Statistical analysis was performed using SPSS 13.0. Stepwise multiple regression analyses were performed to evaluate the correlation between MV parameters and phosphorescence lifetime.

Results

Phosphorescence lifetime in cortical sarcoma

The time-resolved phosphorescence spectra excited by the laser with pulse width of 400 μs show a sharp rise to the peak followed with a slow return to baseline (see Fig. 2), the two lines in Fig. 2 show representative spectra respectively with the shortest lifetime and the longest lifetime. Analyzing the phosphorescence decay traces shown in Fig. 2 using Eq. 2, the decay constants in tumors representing phosphorescence lifetime are respectively 503 and 735 μs. Decay constants from other mice were obtained in a similar way and the decay constants T_s are listed in Table 2.

It can be observed that tumor growth enlarged T_s, starting at an average decay constant of 548 μs, average T_s changes to be 654 μs after 10 days of tumor growth. The decay constants significantly increase with the development of tumors (comparison between the groups, $P<0.05$).

Transplanted tumor growth and angiogenesis

As showed in Table 1, difference of tumor weight between all the animal groups are significant ($P<0.05$). It further indicates tumor weight significantly increases with tumor growth. The digital image analysis reveals MV counts per image and the relative area of all MV per image field (%) also increase with the duration of bearing tumor ($P<0.05$), while no significant different results of the average area of MV per image and the average perimeter of MV per image are detected between the animal groups ($P>0.05$). Pearson correlation analysis indicates MV counts per image, the average area of MV and the relative area of all MV per image field (%) are positively correlative with tumor weight ($r=0.841$, $P<0.01$; $r=0.515$, $P<0.05$; $r=0.893$, $P<0.01$). The tumor microvessel stainings are presented in Fig. 3.

Correlation between angiogenesis and phosphorescence lifetime in tumor progression

Pearson correlation analysis indicates tumor weight, MV counts per image, the average area of MV and the relative area of all MV per image field (%) are positively correlative with the phosphorescence lifetime ($r=0.880$, $P<0.01$; $r=0.935$, $P<0.01$; $r=0.615$, $P<0.05$; $r=0.932$, $P<0.01$).

For the stepwise multiple regression, the tumor weight, MV counts per image, the average area of MV per image, the average perimeter of MV per image, and the relative area of all MV per image field are defined as the independent variables, the phosphorescence decay constant is defined as the dependent variable. Comparing the partial

Table 2 Phosphorescence lifetime and parameters of tumor angiogenesis in the different development courses of transplanted S180 ($x\pm s$)

Course (day)	Phosphorescence decay constant (μs)	MVC (per image)	Average area of vessels (μm^2)	Average perimeter of vessels (μm)	Related area of vessels (%)
5	548±12	4.83±2.04	109.59±29.96	37.25±14.47	1.16±0.41
7	571±16	7.16±2.36	113.37±23.57	36.11±11.28	1.71±0.18
10	606±23	10.44±3.35	107.61±28.34	38.50±28.34	2.51±0.72
12	631±17	11.97±3.16	111.34±19.96	40.25±24.13	3.28±0.27
15	654±15	15.83±4.26	124.42±40.50	36.32±15.03	4.40±0.14

MVC: microvessel count.

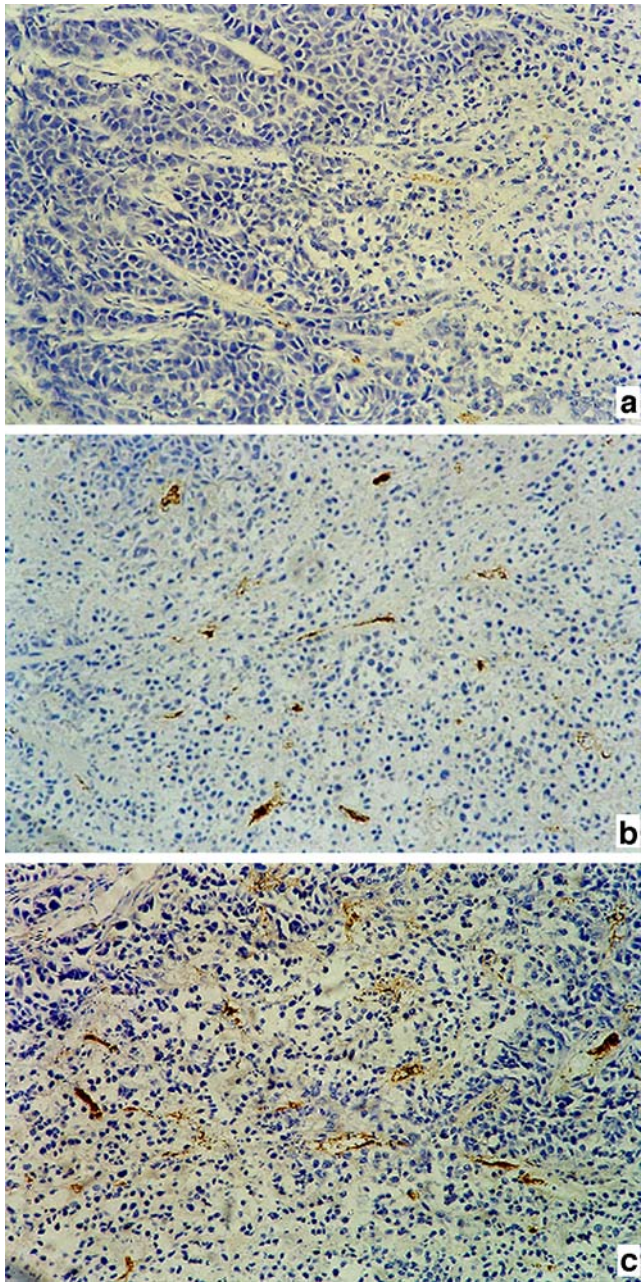

Fig. 3 Microvessels in transplanted S180 respectively at 5th, 10th, 15th day by immunohistochemical staining of FVIII (×200). **a** 5th day, **b** 10th day, **c** 15th day

regression coefficients, the results reveal only the relative area of all MV per image field is included in the regression. Multiple regression procedures estimated a linear equation of the form:

$$\text{Decay Constant} = 521.619 + 30.558 \cdot (\%) \quad (3)$$

The results indicate the relative area of all MV per image field is positively correlative with the phosphorescence decay constant ($P<0.01$; see Fig. 4).

Discussion

Angiogenesis is an early event in tumor progression, investigation of the promotion of angiogenesis is fundamental in the field of tumor prognose. As an indirect measure of angiogenesis, microvessel density has been reported to be a valuable prognostic indicator. Microvessel density is always measured by image analyses of immunohistological sections. As a new attempt to estimate microvessel density, a time-resolved phosphorescence method is proposed in this paper, then, a correlation analysis of the data from the optical method and immunohistochemical examination is conducted to investigate the validity of phosphorescence lifetime in estimating tumor angiogenesis.

In many studies the photosensitizer Pd-TCPP is often used as a reporter of oxygen concentration in tissue. As the oxygen concentration of tumor tissue is higher than that of the adjacent normal tissue [31]. Furthermore, the tumor oxygen decreases with the tumor growing [32, 33]. According to oxygen dependence of the phosphorescence lifetime, the phosphorescence lifetime will presumably increase with the tumor growth. This can explain the experimental result showed in Table 2.

As described in former subsection, substantial increases in tumor mass require an increase of oxygen for energy production and tissue function, lack of an adequate blood supply and increasing distances from existing blood vessels means tumor cells are starved of oxygen, this leads to areas of hypoxia or even anoxia in the tumor. In response to hypoxia, tumors secrete angiogenic growth factors to stimulate vessel growth and oxygen delivery. This is mediated by a hypoxia inducible factor (HIF-1) [34], which modulates the expression of a number of hypoxia inducible genes and angiogenic factors such as VEGF. However, the oxygen pressure continuously decreases with increasing tumor size despite increases in microvessel density. So, there is presumably a negative correlation between oxygen pressure and angiogenesis in tumor progression. This becomes the foundation for our work.

For an ideal optical method, excitation pulse is essential for reliable and precise phosphorescence measurement in tumor tissue. As phosphorescence spectra shown in Fig. 2 are consistent with previous time-resolved phosphorescence spectra measurements, [35, 36] semiconductor laser of 400 μs pulse width is used as excitation source.

By the application of computer-assisted, quantitative image analyses of immunohistochemical sections, the present study has demonstrated three parameters of vascularity (specially, MV counts per image and the relative area of all MV per image) significantly increase with the development of the tumor.

Before we conducted correlation analysis, a scatter plot was created. Through scatter plot, we can determine

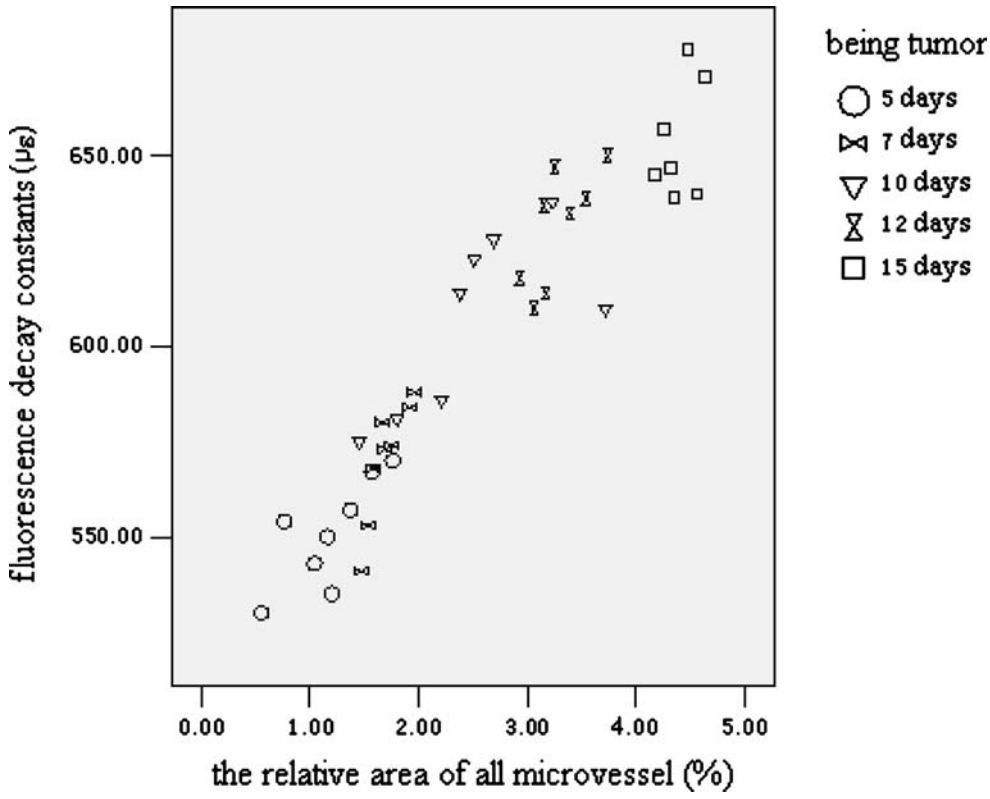

Fig. 4 Scatter plot of the relationship between the relative area of all MV per image field and phosphorescence decay constants

whether a linear relationship exists between tumor angiogenesis and phosphorescence lifetime. After the correlation analysis in tumor progression, the tumor weight, MV counts per image, the average area of MV and the relative area of all MV per image field are found positively correlative with the phosphorescence lifetime. Furthermore, a linear equation is estimated to describe the correlation between microvessel density and phosphorescence lifetime, in which the relative area of all MV per image is included as independent variable, while MV counts per image are excluded because of the positive correlation between MV counts and the relative area of all MV. In addition, no significant increase of the average perimeter and the average area of MV per image with increasing tumor size explained the exclusion of these vascularity parameters in the equation. The linear equation gives a possibility to estimate tumor angiogenesis by the oxygen dependent phosphorescence quenching method.

Conclusion

In this paper, we proposed a time-resolved phosphorescence quenching method and immunohistochemical examination to investigate the correlation between tumor angiogenesis and phosphorescence lifetime in its progression. Results reveal that the decay constant in tumor tissue is enlarged with increasing of tumor size, furthermore, the phosphorescence lifetime is found positively correlative with microvessel density in tumors. It is concluded the phosphorescence lifetime is a valuable indicator of tumor angiogenesis during the tumor development.

Acknowledgements The work was supported by Shenzhen Science and Technology Program (No.200519).

References

1. Folkman J (1990) What is the evidence that tumors are angiogenesis dependent. J Natl Cancer Inst 82(1):4–6
2. Bouck N (1990) Tumor angiogenesis: the role of oncogenes and tumor suppressor genes. Cancer Cells 2:179–185
3. Folkman J, Watson K, Ingber D, Hanahan D (1989) Induction of angiogenesis during the transition from hyperplasia to neoplasia. Nature 339:58–61
4. Weidner N, Semple JP, Welch WR (1991) Tumor angiogenesis and metastasis: correlation in invasive breast carcinoma. N Engl J Med 324(1):1–8
5. Weidner N, Folkman J, Pozza F, Bevilacqua P, Allred EN, Moore DH, Meli S, Gasparini G (1992) Tumor angiogenesis: a new significant and independent prognostic indicator in early-stage breast carcinoma. J Natl Cancer Inst 84:1875–1887
6. Feng BC, Liu KL (1991) A morphological study of stromal microvasculature of nasopharyngeal precancerous lesions. Chin Med J 104:422–424
7. Wesseling P, Laak JAWM, Leeuw HD, Rutter DJ, Burger PC (1994) Quantitative immunohistological analysis of the

microvasculature in untreated human glioblastoma multiforme. J Neurosurg 81:902–909
8. Fox SB, Leek RD, Weekes MP, Whitehouse RM, Gatter KC, Harris AL (1995) Quantitation and prognostic value of breast cancer angiogenesis: comparison of microvessel density, chalkley count, and computer image analysis. J Pathol 177:275–283
9. Zeng H, MacAulay C, Palcic B, Mclean DI (1993) A computerized autofloruescence and diffuse reflectance spectroanalyser for in vivo skin studies. Phys Med Biol 38:231–240
10. Zeng H, MacAulay C, McLean DI, Palcic B (1993) Novel microspectrophotometer and its biomedical applications. Opt Eng 32(8):1809–1813
11. Alfano RR, Tang GC, Pradhan A, Lam W (1987) Fluorescence spectra from cancerous and normal human breast and lung tissues. IEEE J Quantum Electron QE-23:1806–1811
12. Ramanujam N, Mitchell MF, Mahadevan A, Thomsen S, Malpica A, Wright T, Atkinson A, Richards-Kortum RR (1996) Development of a multivariate statistical algorithm to analyze human cervical tissue fluorescence spectra acquired in vivo. Lasers Surg Med 19(1):46–62
13. Schomacker KT, Frisoli JK, Compton CC, Flotte TJ, Richter JM, Nishioka NS, Deutsch TF (1992) Ultraviolet laser-induced fluorescence of colonic tissue: basic biology and diagnostic potential. Lasers Surg Med 12:63–78
14. Panjehpour M, Overholt BF, Schmidhammer JL, Farris C, Buckley PF, Vo-Dinh T (1995) Spectroscopic diagnosis of esophageal cancer: new classification model, improved measurement system. Gastrointest Endosc 45:577–581
15. Bottiroli G, Croce AC, Locatelli D, Nano R, Giombelli E, Messina A, Benericetti E (1998) Brain tissue autofluorescence: an aid for intraoperative delineation of tumor resection margins, Cancer detection. Prevent 22(4):330–339
16. Lakowicz J (1983) Principles of fluorescence spectroscopy. Plenum, New York
17. Schomacker KT, Frisoli JK, Compton CC, Flotte TJ, Richter JM, Deutsch TF (1992) Ultraviolet laser-induced fluorescence of colonic polyps. Gastroenterology 102:1155–1160
18. Wilson DF, Cerniglia GJ (1994) Oxygenation of tumors as evaluated by phosphorescence imaging. Adv Exp Med Biol 345:539–547
19. Wilson DF, Vinogradov S, Lo LW, Huang L (1996) Oxygen dependent quenching of phosphorescence: a status report. Adv Exp Med Biol 388:101–107
20. Wilson DF, Vinogradov SA (1994) Recent advances in oxygen measurements using phosphorescence quenching. Adv Exp Med Biol 361:61–66
21. Zheng L, Golub AS, Pittman RN (1996) Determination of PO2 and its heterogeneity in single capillaries. Am J Physiol 271(Heart Cire. Physiol. 40):H365–H372
22. Sinaasappel M, Ince C (1996) Calibration of Pd-porphyrin phosphorescence for oxygen concentration measurements in vivo. J Appl Physiol 81(5):2297–2303
23. Lee SK, Shin YB, Pyo HB, Park SH, Ogura SI, Okura I (2001) Measurement of oxygen concentrations in tumor cells by the phosphorescence quenching method. Bull Korean Chem Soc 22 (3):259–260
24. Hansen-Algenstaedt N, Stoll BR, Padera TP, Dolmans DEJ, Hicklin DJ, Fukumura D, Jain RK (2000) Tumor oxygenation in hormone-dependent tumors during vascular endothelial growth factor receptor-2 blockade, hormone ablation, and chemotherapy. Cancer Res 60:4556–4560
25. Vaupel P, Kallinowski F, Okunieff P (1989) Blood flow, oxygen and nutrient supply, and metabolic microenvironment of human tumors: a review. Cancer Res 49:6449–6465
26. Helmlinger G, Yuan F, Dellian M, Jain RK (1997) Interstitial pH and pO2 gradients in solid tumors in vivo: high-resolution measurements reveal a lack of correlation. Nat Med 3: 177–182
27. Brown JM, Giaccia AJ (1998) The unique physiology of solid tumors: opportunities (and problems) for cancer therapy. Cancer Res 58:1408–1416
28. Shweiki D, Itin A, Soffer D, Keshet E (1992) Vascular endothelial growth factor induced by hypoxia may mediate hypoxia-initiated angiogenesis. Nature 359:843–845
29. Fukumura D, Xavier R, Sugiura T, Chen Y, Park EC, Lu N, Selig M, Nielsen G, Taksir T, Jain RK, Seed B (1998) Tumor induction of VEGF promoter activity in stromal cells. Cell 94:715–725
30. Qian CN, Min HQ, Liang XM (1997) Primary study of neovasculature correlating with metastatic nasopharyngeal carcinoma using computer image analysis. J Cancer Res Clin Oncol 123 (11–12):645–651
31. Braun RD, Lanzen JL, Snyder SA, Dewhirst MW (2001) Comparison of tumor and normal tissue oxygen tension measurements using OxyLite or microelectrodes in rodents. Am J Physiol 280:H2533–H2544
32. Dewhirst MW, Ong ET, Klitzman B, Secomb TW, Vinuya RZ, Dodge R, Brizel D, Gross JF (1992) Perivascular oxygen tensions in a transplantable mammary tumor growing in a dorsal flap window chamber. Radiat Res 130:171–182
33. Dewhirst MW, Ong ET, Braun RD, Smith B, Klitzman B, Evans SM, Wilson D (1999) Quantification of longitudinal tissue PO2 Gradients in widow chamber tumours: impact of tumour hypoxia. Br J Cancer 79:1717–1722
34. Byrne M, Bouchier-Hayes DJ, Harmey JH (2005). Angiogenic and cell survival functions of vascular endothelial growth factor (VEGF). J Cell Mol Med 9(4):777
35. Pitts JD, Mycek MA (2001) Design and development of a rapid acquisition laser-based fluorometer with simultaneous spectral and temporal resolution. Rev Sci Instrum 72(7):3061–3072
36. Vishwanath K, Pogue B, Mycek MA (2002) Quantitative fluorescence lifetime spectroscopy in turbid media: comparison of theoretical, experimental and computational methods. Phys Med Bio 47:3387–3405